J Fluoresc (2013) 23:697–703
DOI 10.1007/s10895-013-1189-7

ORIGINAL PAPER

A Graphene Oxide–Based Sensing Platform for The Label-free Assay of DNA Sequence and Exonuclease Activity via Long Range Resonance Energy Transfer

Yixuan Jiang · Jianniao Tian · Sheng Chen · Yanchun Zhao · Yuan Wang · Shulin Zhao

Received: 20 July 2012 / Accepted: 24 February 2013 / Published online: 9 March 2013

Abstract Graphene oxide (GO) was introduced as an efficient quencher for label-free and sensitive detection of DNA. Probe DNA (pDNA) was mixed with ethidium bromide (EB) and graphene oxide (GO). The interaction between EB and GO led to the fluorescent quenching. Upon the recognition of the target, EB was intercalated into duplex DNA and kept away from GO, which significantly hindered the long range resonance energy transfer (LrRET) from EB to GO and, thus, increased the fluorescence of EB. The changes in fluorescent intensity produced a novel method for sensitivity, and specificity detection of the target. Based on the structure-switching of aptamers, this strategy could be conveniently extended for detection of other biomolecules, which had been demonstrated by the detection of exonuclease activity.

Keywords · Graphene oxide (GO) · The long range resonance energy transfer (LrRET) · Exonuclease activity · DNA

Abbreviations

GO	Graphene oxide
pDNA	Probe DNA
EB	Ethidium bromide
LrRET	Long range resonance energy transfer
Exo III	Exonuclease
tDNA	Target DNA

Y. Jiang · J. Tian (✉) · S. Chen · Y. Zhao · Y. Wang · S. Zhao
Key Laboratory for the Chemistry and Molecular Engineering of Medicinal Resources (Ministry of Education of China), College of Chemistry and Chemical Engineering of Guangxi Normal University, Guilin 541004, China
e-mail: tianjn58@yahoo.com.cn

Introduction

Graphene is a single-atom-thick and two-dimensional nanomaterial, which has recently attracted an increasing interest. Because of its high mechanic strength, superior electric conductivity and excellent thermal properties [1–4], graphene has attracted wide research in different fields. In addition, a large surface area and surface functionalities of graphene make it possible to be chemical and biological sensors [5, 6]. To improve its solubility in water, graphene is oxidized to graphene oxide (GO) by generating surface carboxylic acid and hydroxyl groups. Previously, GO was reported to adsorb strongly with single-stranded nucleic acids through π-π stacking interaction between the ring structures in the nucleobases and the hexagonal cells of GO [7]. Based on this theory, many GO-based DNA sensors have been constructed for the detection of nucleic acid [8], proteins [9, 10], and small molecules [11–13]. In most of these previous studies, GO as an excellent energy acceptor can efficiently quench the fluorescence of nearby organic dyes over a wide wavelength range. Different way from fluorescence resonance energy transfer(FRET), GO can quench organic dyes based on long range resonance energy transfer(LrRET) [14]. The energy transfers rate of dye to GO is $(R)^{-4}$, where R is the relative distance between the donor and the acceptor, indicating that GO could be more efficiently quench the fluorescence of dyes molecule.

However, the above-mentioned GO-based DNA sensors usually render several limitations such as high-cost, and time-consuming fluorescence labeling and multiple steps of chemical modification. In order to overcome these shortcomings, we have introduced ethidium bromide (EB) as a model, a dye known to specifically intercalates with double-

stranded DNA [15], to build up an inexpensive and label-free biosensor. We describe a convenient but effective platform for DNA detection based on LrRET between EB and GO. The method is also applicable to other DNA-intercalating dyes, such as GeneFinder™, SYBR Green I, GoldView™ etc.

By introducing GO as signal-to-background ratio enhancer in this contribution,sensitive detection of DNA was achieved. Compared to the traditional methods, the strategy is convenient and cost-saving. On the other hand, detection of exonuclease was performed to test the practicality of this platform. Exonucleases are DNA-degrading enzymes that play important roles in a variety of physiological and cellular processes. In recent years, Exo III, which can selectively digests the 3′-end of nucleic acid strands in duplex DNAs, is widely used as an amplifying biocatalyst in the detection of analytes [16, 17]. As the results show, through this platform, rapid qualitative and quantitative detection of Exo III can be carried out, indicating that this method can be developed for other physiologically active substances.

Experimental

Materials

Ethidium bromide (EB) was purchased from Sigma-Aldrich (China). Graphene oxide (GO) were brought from Chengdu Organic Chemicals Co. Ltd, Chinese Academy of Sciences (Chengdu, China). Probe DNA (pDNA) 5′-CGCAATATGGATGAAGAACTAC-3′, target DNA (tDNA) 5′-GTAGTTCTTCATCCATATTGCG-3′ and Mismatched DNA (mDNA) 5′-ACGAGGTGGATCAACACCCATA-3′ were synthesized by Shanghai Sangon Biotechnology Co.Ltd (Shanghai, China). Exo III was purchased from Shanghai Sangon Biotechnology Co.Ltd (Shanghai, China).

Fluorescence spectra were measured with an LS-55 luminescence spectrometer (Perkin Elmer, USA).

Methods

Detection of DNA

In a typical DNA assay, the probe DNA was hybridized with the target DNA in 66 mM Tris–HCl (pH7.4) buffer solution containing 10 mM NaCl. The solution was heated to 90°C for 5 min and then slowly cooled down to room temperature to ensure that nucleic acids were hybridized. Then 40 μg/L of EB was added and incubated at room temperature for 15 min. At last 0.12 mg/mL GO was added and incubated for further 10 min, and then the mixture was transferred for fluorescence measurements by an LS-55 luminescence with an excitation wavelength of 480 nm.

Exonuclease Activity Assay

To prepare duplex DNA, probe DNA was mixed with complementary strand target DNA (1:1) in DNA hybridization

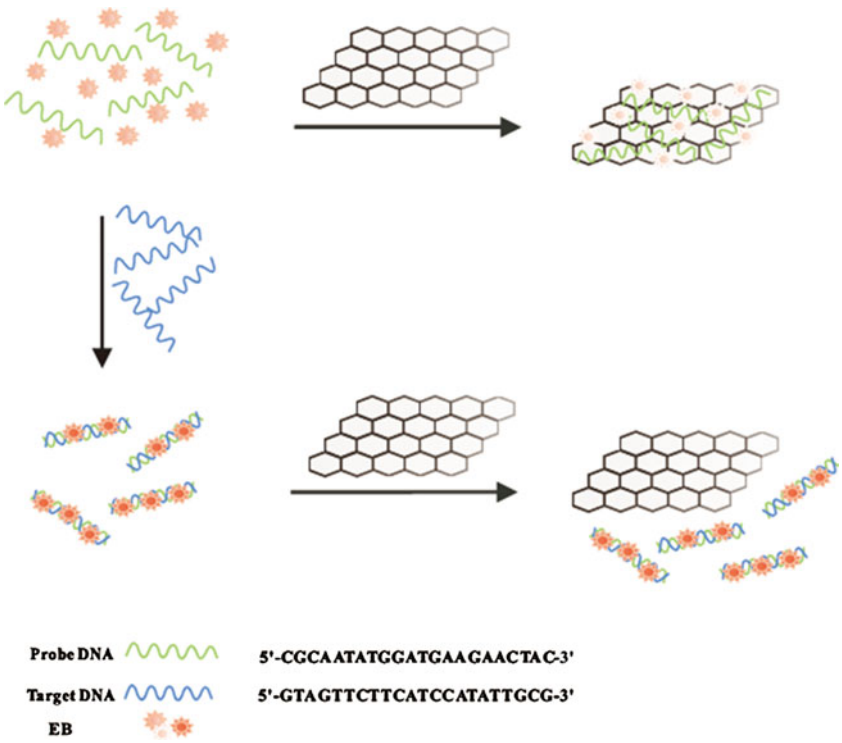

Scheme 1 Principle of the DNA detection system based on the EB-GO/label-free DNA LrRET

buffer, heated to 90°C for 5 min followed by slow cooling to room temperature. The obtained dsDNA solution was stored at 4 °C for further use. Exo III and 2 μM of dsDNA were added to the reaction buffer and incubated at 37°C for 1 h, then added 40 μg/L EB at room temperature for 15 min. After the additions of 0.12 mg/mL GO for 10 min, the fluorescence of the mixture was measured at 605 nm with the excitation of 480 nm at room temperature.

Exonuclease Inhibition Assay

In the inhibition experiment, to evaluate the effects of inhibitors on Exo III digestion process, EDTA (0.1–2.0 mM)

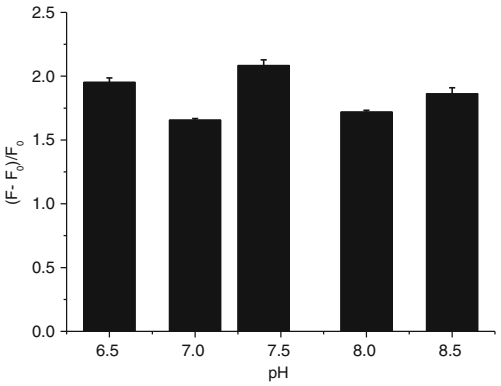

Fig. 2 Effect of pH on the fluorescence changes. Concentrations: [pDNA]=3 μM, [tDNA]=800 nM, [EB]=40 μg/L, [GO]=0.12 mg/mL, [Na^+]=10 mM. All data were collected from three measurements, and the error bars indicate the standard deviation

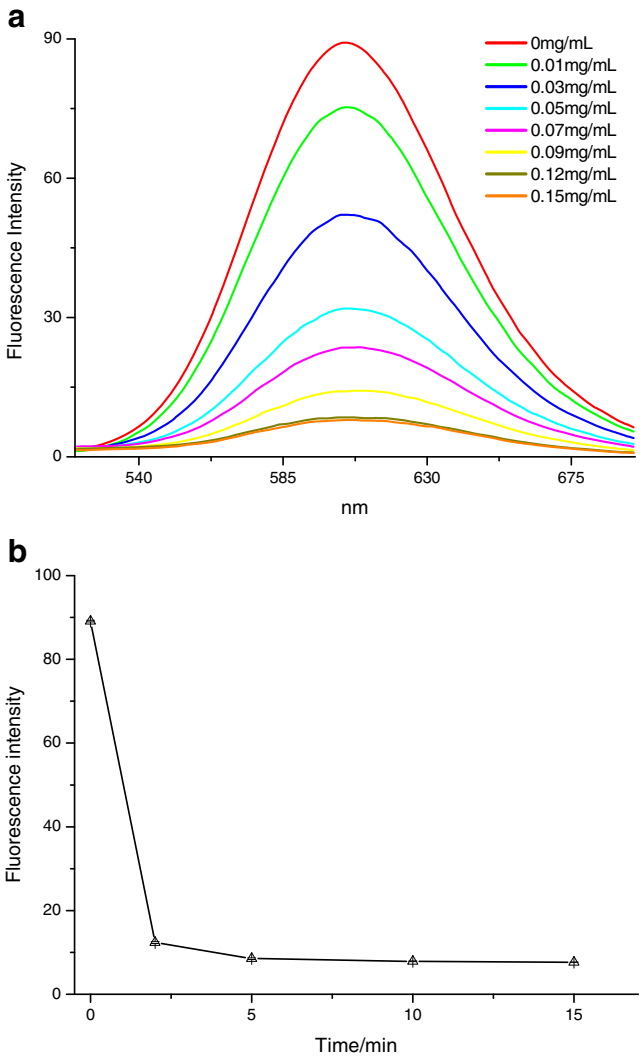

Fig. 1 **a** Fluorescence spectra of 40 μg/L EB after incubation with different amounts of GO (top to bottom: 0, 0.01, 0.03, 0.05, 0.07, 0.09, 0.12, 0.15 mg/mL) for 10 min. **b**Fluorescence intensities of 40 μg/L EB via time in the presence of 0.12 mg/mL GO. The assays were all carried out in the Tris–HCl buffer (pH7.4) containing 3 μM pDNA. All data were collected from three measurements, and the error bars indicate the standard deviation

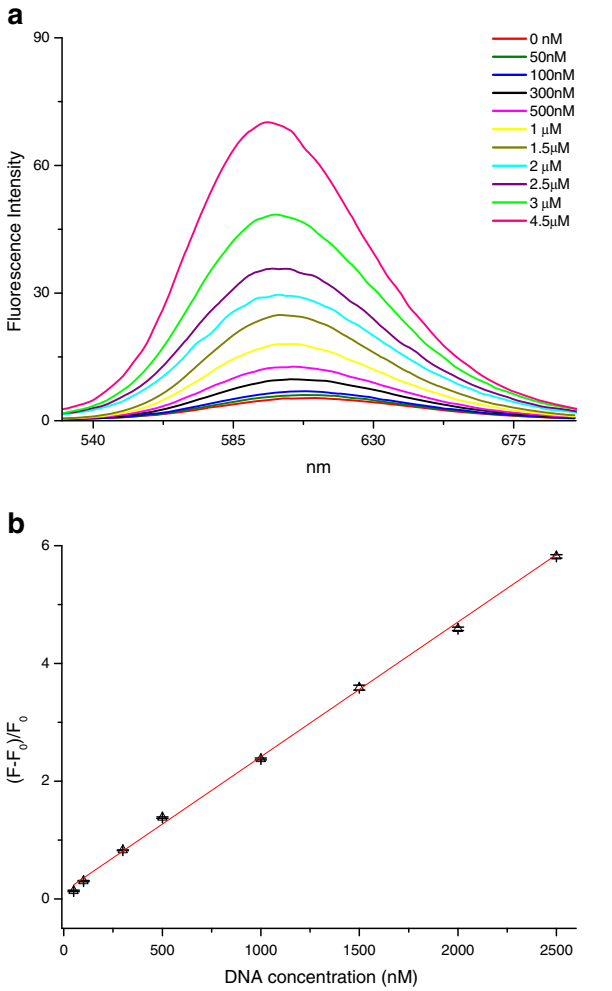

Fig. 3 **a** Fluorescent spectra of pDNA-EB/GO with various concentrations of tDNA. **b** Plot of the values of $(F-F_0)/F_0$ for pDNA-EB/GO with respect to the concentrations of tDNA (50–2,500 nM). Concentrations: [pDNA]=3 μM; tDNA 0, 50, 100, 300, 500, 1,000, 1,500, 2,000, 2,500, 3,000, 4,500 nM; [EB]=40 μg/L, [GO]=0.12 mg/mL. All data were collected from three measurements, and the error bars indicate the standard deviation

was contained in the reaction buffer. After the addition of 2 μM dsDNA and 25 U/mL Exo III, the reaction was performed at 37 °C for 1 h. The fluorescence of the mixture was measured at 605 nm with the excitation of 480 nm at room temperature.

Results and Discussion

The Principle of LrRET between GO and EB

The working principle of the label-free detection DNA is schematically represented in Scheme 1. Before target DNA binding, both probe DNA and EB are adsorbed on the surface of GO, and the fluorescence of EB is quenched by GO following LrRET process. In the presence of target DNA, however, the formation of duplex DNA via hybridization leads to EB intercalation, and reduces the π–π stacking and hydrogen bonding interaction between GO and DNA [18]. EB keep away from GO, and fluorescence recovery gradually. So, by observing the change of fluorescence intensity, we can detect the concentration of target DNA.

The Optimization of Experimental Conditions

To evaluate the fluorescence quenching of EB on the GO surface, 40 μg/L EB, and 3 μM pDNA were prepared in the Tris–HCl buffer (pH7.4). After the addition of a different amount of GO (0, 0.01, 0.03, 0.05, 0.07, 0.09, 0.12, 0.15 mg/mL) for 10 min, fluorescence emission spectra were used to investigate the fluorescence quenching of dye, resulting from the interaction between EB and GO. As shown in Fig. 1a, EB exhibited strong fluorescence emission around 605 nm in the absence of GO. However, the fluorescence intensity gradually decreased with the increased of GO concentration. Up to 91 % of original fluorescence emission was quenched upon the addition of 0.12 mg/mL GO within 10 min. The fact is attributed to the adsorption of EB on GO surface via the strong π-π stacking and electrostatic interaction, highly efficient LrRET between EB and GO can occur, thus causing a quenching of the EB fluorescence. In the presence of 0.12 mg/mL GO, fluorescence intensity of EB trended to a minimum value. Thus, 0.12 mg/mL GO was used for analytical purposes.

The effect of incubation time was also investigated. Figure 1b displays the changes of fluorescence intensity with incubation time. It was observed that the fluorescence signal decreased gradually with the increased of the reaction time and then reached equilibrium in 10 min. Thus, the optimal reaction time was chosen to be 10 min.

Since the pH was an important factor influencing the quenching ability of GO, we explored the effect of the pH. In the optimized assay, 3 μM pDNA and 800 nM tDNA were put into 66 mM Tris–HCl buffer. After the incubation at 90°C for 5 min and then slowly cooled down to room temperature, 40 μg/L EB was added into the reaction mixture for 15 min. 0.12 mg/mL GO was added and incubated for further 10 min, followed by the fluorescence measurement with the excitation wavelength of 480 nm. From the results of Fig. 2, $(F- F_0)/F_0$ was the change of EB fluorescence intensity before and after addition of 0.12 mg/mL GO. To get a high signal to backgroud, the optimal pH was 7.4 in these experiments.

The Detection of tDNA

Under optimal conditions, with the increasing concentration of tDNA used for hybridization prior to addition of GO, the

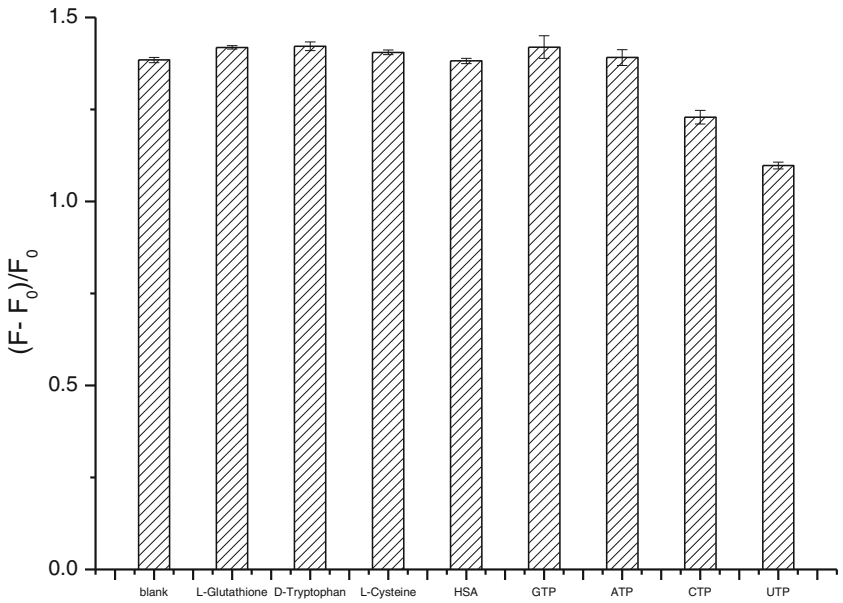

Fig. 4 Changes of pDNA-EB/GO fluorescence intensity incubated in the presence of 500 nM tDNA with 66 mM Tris–HCl buffer pH 7.4 containing 10 mM NaCl (blank), L-Glutathione, D-Tryptophan, L-Cysteine, HSA, GTP, ATP, CTP and UTP. Concentrations: [pDNA]= 3 μM; [tDNA]=500 nM; [EB]=40 μg/L; [GO]=0.12 mg/mL; Interfering substances 1 μM (66 mM Tris–HCl buffer pH7.4 containing 10 mM NaCl). All data were collected from three measurements, and the error bars indicate the standard deviation

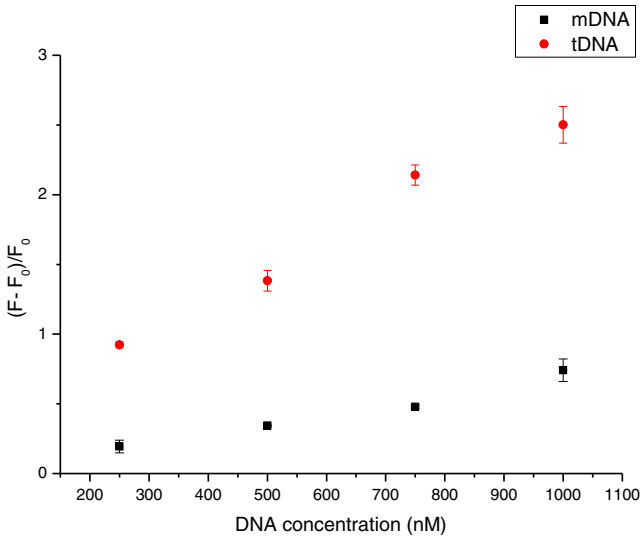

Fig. 5 Changes of pDNA-EB/GO fluorescence intensity incubated with various concentrations of tDNA or mDNA in 66 mM Tris–HCl buffer pH 7.4 containing 10 mM NaCl. Concentrations: [pDNA]= 3 μM; tDNA 250, 500, 750, 1,000 nM; mDNA 250, 500, 750, 1,000 nM; [EB]=40 μg/L; [GO]=0.12 mg/mL; All data were collected from three measurements, and the error bars indicate the standard deviation

fluorescence intensity increased (Fig. 3a). The results showed that the formation of double-stranded structure made EB intercalation, and protected EB from GO. The regression equation was $y = (0.002 \pm 9.120 \times 10^{-6}) \times + (0.126 \pm 0.005)$. A linear correlation ($R^2$=0.996) (Fig. 3b) existed between the value of (F- F_0)/F_0 and the concentration of tDNA over the range of 50–2,500 nM, where F_0 and F were the fluorescence intensity of the solution without and with the addition of tDNA. The limit of detection (LOD) for DNA was 32 nM at a signal-to-noise of 3.

Further investigation was made in the presence of several interfering substances. It can be seen from Fig. 4, due to the stable dsDNA structure between the pDNA and perfectly complementary tDNA, the (F- F_0)/F_0 did not change significantly even if the presence of interfering substances. It indicated that the method has good selectivity. We also investigated the specificity of this method. Mismatched DNA (mDNA) as the targets was employed for the hybridization detection (Fig. 5). Although the (F- F_0)/F_0 value of EB increased along with concentration of mDNA increased, but this change is very small compared to the tDNA, indicating that our strategy has a good specificity.

The Detection of Exonuclease and Inhibitor

To demonstrate the extended practicality of the proposed approach, detection of Exonuclease was performed. Exo III was added to a mixture of dsDNA and EB in which the dsDNA exhibits high fluorescence. The fluorescence was greatly quenched after the addition of GO originated from the strong adsorption of DNA fragments on GO and the effective LrRET between EB and GO. Thus the activity of

Scheme 2 Principle of the Exo III detection system based on the EB-GO/label-free DNA LrRET

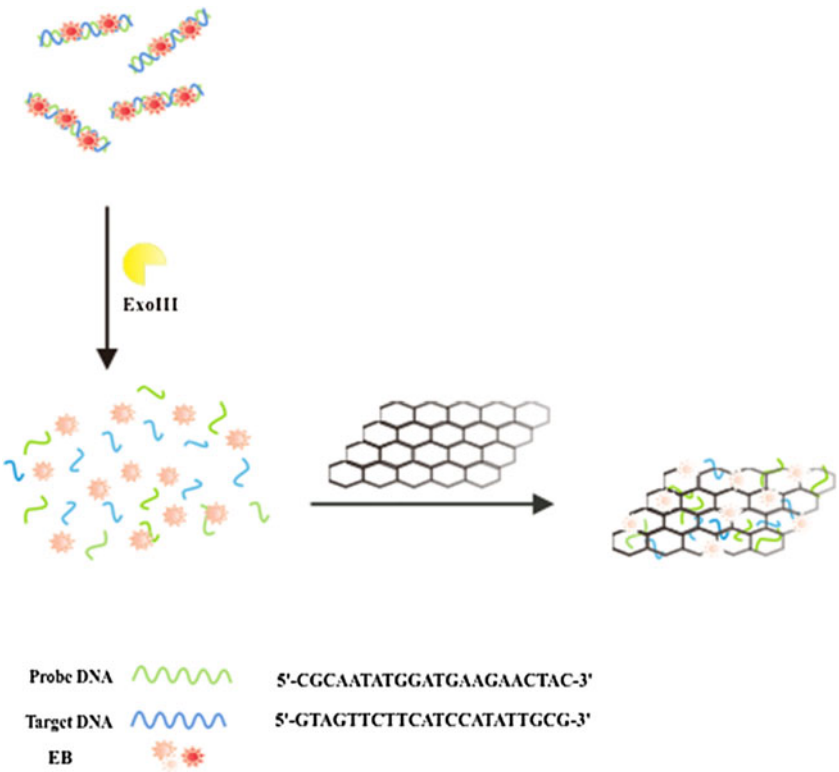

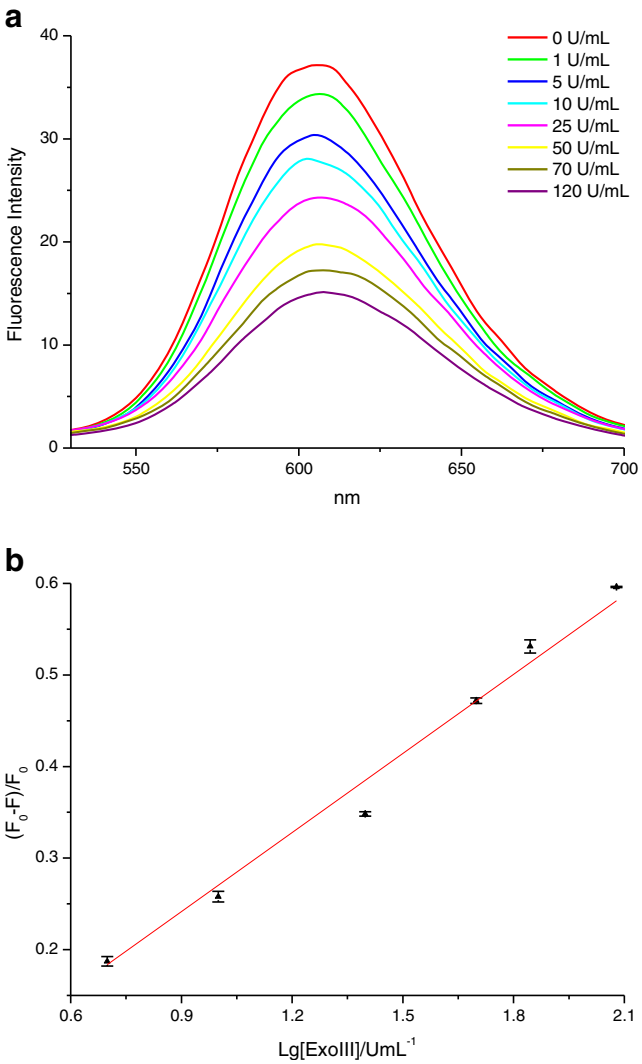

Fig. 6 **a** Fluorescent spectra of dsDNA-EB/GO with various concentrations of Exo III. **b** Plot of the values of $(F_0\text{-}F)/F_0$ for dsDNA-EB/GO with respect to the logarithm of the concentrations of Exo III (5–120 U/mL). Concentrations: [dsDNA]=2 μM; [EB]=40 μg/L; [GO]=0.12 mg/mL; Exo III 0, 1, 5, 10, 25, 50, 70, 120 U/mL. All data were collected from three measurements, and the error bars indicate the standard deviation

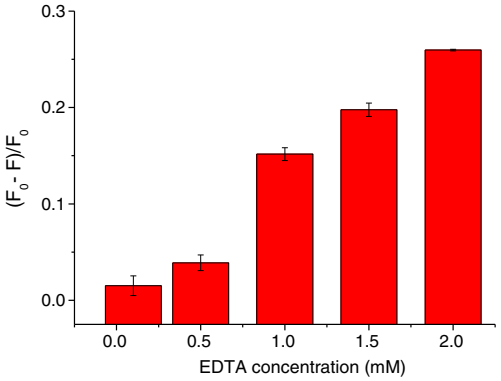

Fig. 7 Inhibition of Exo III by EDTA (0.1, 0.5, 1.0, 1.5, 2.0 mM). Concentrations: [dsDNA]=2 μM; [EB]=40 μg/L; [GO]=0.12 mg/mL; Exo III: 25 U/mL. All data were collected from three measurements, and the error bars indicate the standard deviation

Exo III can be easily reflected by the fluorescence signal changes (Scheme 2).

Figure 6(a) revealed that the fluorescence of the dsDNA-EB/GO decreased upon increasing the concentration of Exo III up to 120 U/mL because the digestion of the 3′-end of nucleic acid strands in duplex DNAs by Exo III caused the release of EB. DNA fragments and EB were adsorbed on the surface of GO, and the fluorescence of EB was quenched by GO following LrRET process. All the experiments were finished in 90 min. This method is much more efficient than the traditional methods [9]. There was a good linear relationship (R^2=0.992) between the value of $(F_0\text{- }F)/F_0$ and the logarithm of the concentration of Exo III over the range of 5–120 U/mL (Fig. 6b). The regression equation was $y = (0.288 \pm 0.002) \times +(-0.018 \pm 0.002)$ and the LOD of Exo III was 1 U/mL at a signal-to-noise of 3.

We know that the active center of enzymes usually contain metal ions. EDTA can form complexes with metal ions, thereby reducing the concentration of metal ions, the enzyme lost activity [19, 20]. The inhibition effect of EDTA was investigated through the proposed detection platform. Figure 7 showed that fluorescence intensity increased with an increasing concentration of EDTA, indicating that Exo III degradation ability was weakened in the presence of EDTA. Merely 0.1 mM EDTA had led to an obvious inhibition effect on Exo III. These results suggested the potential use of the present assay for the studies of exonuclease inhibition.

Conclusion

We have designed a sensitive and selective platform for detection of DNA. In this platform, GO plays a very important role to enhance the signal to noise ratio for DNA detection with EB. Further, the potential application of the platform for studies of exonuclease and exonuclease inhibition has also been shown. The advantages of this method are obvious. At first, it avoids the need to design complicated fluorescent aptasensors and use of labeled aptamer, cost less time and more effective. Second, GO has a high LrRET efficiency, greatly reducing the fluorescence background signal. In addition, compared with other fluorescent quenchers, GO can be prepared at very low cost. Last, this method can in principle be used to detect different analytes by designing different aptamer based on the structure-switching of aptamers.

Acknowledgments This work has been supported by National Natural Science Foundation of China (No. 21165004, 21163002), the Guangxi Natural Science Foundation of China (2010GXNSFF013001, 2012GXNSFBA053022), Innovation Plan in Graduate Education of

Guangxi Province (2010106020703 M70) and the project of Key Laboratory for the Chemistry and Molecular Engineering of Medicinal Resources(Guangxi Normal University), Ministry of Education of China(CMEMR2011-14).

References

1. Dikin DA, Stankovich S, Zimney EJ, Piner RD, Dommett GHB, Evmenenko G, Nguyen ST, Ruoff RS (2007) Preparation and characterization of graphene oxide paper. Nature 448:457–460
2. Geim AK, Novoselov KS (2007) The rise of graphene. Nat Mater 6:183–191
3. Yang W, Ratinac KR, Ringer SP, Thordarson P, Gooding JJ, Braet F (2010) Carbon nanomaterials in biosensors: should you use nanotubes or graphene? Angew Chem Int Ed 49:2114–2138
4. Novoselov KS, Geim AK, Morozov SV, Jiang D, Zhang Y, Dubonos SV, Grigorieva IV, Firsov AA (2004) Electric field effect in atomically thin carbon films. Science 306:666–669
5. Liu LH, Lerner MM, Yan M (2010) Derivitization of pristine graphene with well-defined chemical functionalities. Nano Lett 10:3754–3756
6. Li J, Lu CH, Yao QH, Zhang XL, Liu JJ, Yang HH, Chen GN (2011) A graphene oxide platform for energy transfer-based detection of protease activity. Biosens Bioelectron 26:3894–3899
7. Varghese N, Mogera U, Govindaraj A, Das A, Maiti PK, Sood AK, Rao CNR (2009) Binding of DNA nucleobases and nucleosides with graphene. Chem Phys Chem 10:206–210
8. Dong H, Gao W, Yan F, Ji H, Ju H (2010) Fluorescence resonance energy transfer between quantum dots and graphene oxide for sensing biomolecules. Anal Chem 82:5511–5517
9. Jang H, Kim YK, Kwon HM, Yeo WS, Kim DE, Min DH (2010) A graphene-based platform for the assay of Duplex-DNA unwinding by helicase. Angew Chem Int Ed 49:5703–5707
10. Bi S, Zhao T, Luo B (2012) A graphene oxide platform for the assay of biomolecules based on chemiluminescence resonance energy transfer. Chem Commun 48:106–108
11. Song YJ, Qu KG, Zhao C, Ren JS, Qu XG (2010) Graphene oxide: intrinsic peroxidase catalytic activity and its application to glucose detection. Adv Mater 22:2206–2210
12. Zhang C, Yuan Y, Zhang S, Wang Y, Liu Z (2011) Biosensing platform based on fluorescence resonance energy transfer from upconverting nanocrystals to graphene oxide. Angew Chem Int Ed 50:6851–6854
13. Liu C, Wang Z, Jia H, Li Z (2011) Efficient fluorescence resonance energy transfer between upconversion nanophosphors and graphene oxide: a highly sensitive biosensing platform. Chem Commun 47:4661–4663
14. Swathi RS, Sebastian KL (2009) Long range resonance energy transfer from a dye molecule to graphene has $(\text{distance})^{-4}$ dependence. J Chem Phys 130:86–101
15. He F, Tang Y, Yu M, Feng F, An L, Sun H, Wang S, Li Y, Zhu D, Bazan GC (2006) Quadruplex-to-duplex transition of g-rich oligonucleotides probed by cationic water-soluble conjugated polyelectrolytes. J Am Chem Soc 128:6764–6765
16. Freeman R, Liu X, Willner I (2011) Amplified multiplexed analysis of DNA by the exonuclease iii-catalyzed regeneration of the target DNA in the presence of functionalized semiconductor quantum dots. Nano Lett 11:4456–4461
17. Chen H, Wang J, Liang G, Zhang P, Kong JL (2012) A novel exonuclease III aided amplification method for sensitive nucleic acid detection based on single walled carbon nanotube induced quenching. Chem Commun 48:269–271
18. Yang X, Zhang X, Liu Z, Ma Y, Huang Y, Chen Y (2008) High-efficiency loading and controlled release of doxorubicin hydrochloride on graphene oxide. J Phys Chem C 1121:7554–7558
19. Chen Q, Zhang W, Wang H, Zhou H (1996) Kinetics of inactivation of green crab (*Scylla Serrata*) alkaline phosphatase during removal of zinc ions by ethylenediaminetetraacetic acid disodium. Int J Biol Macromol 19:257–261
20. Whisnant A, Gilman S (2002) Studies of reversible inhibition, irreversible inhibition, and activation of alkaline phosphatase by capillary electrophoresis. Anal Biochem 307:226–234